Ab initio description of nonlinear dynamics of coupled microdisk resonators with application to self-trapping dynamics

Hamidreza Ramezani,[1] Tsampikos Kottos,[1,3] V. Shuvayev,[2] and L. Deych[2]
[1]*Department of Physics, Wesleyan University, Middletown, Connecticut 06459, USA*
[2]*Department of Physics, Queens College of the City University of New York (CUNY) Flushing, New York 11367*
[3]*Max-Planck-Institut für Dynamik und Selbstorganisation, Göttingen, Germany*
(Received 1 November 2010; published 27 May 2011)

An *ab initio* approach is used to describe the time evolution of the amplitudes of whispering gallery modes in a system of coupled microdisk resonators with Kerr nonlinearity. It is shown that this system demonstrates a transition between Josephson-like nonlinear oscillations and self-trapping behavior. Manifestation of this transition in the dynamics of radiative losses is studied.

DOI: 10.1103/PhysRevA.83.053839 PACS number(s): 42.60.Da, 42.55.Sa, 42.65.Sf

I. INTRODUCTION

Whispering gallery modes (WGMs) are optical excitations that exist in axially symmetrical optical resonators. In the geometric optic framework they can be described as waves propagating at large incidence angles along the surface of the resonator and trapped in an optical potential arising due to total internal reflection. Due to high Q factors and small mode volumes of WGMs, one should expect a significant enhancement of nonlinear effects in such structures [1–3]. Indeed, a variety of nonlinear phenomena such as ultralow threshold Raman lasing [4], parametrical optical oscillations [5], and optical comb generation [6] have been experimentally demonstrated in WGM resonators. Theoretical understanding of these effects, however, relied mostly either on purely phenomenological approaches similar to that of Ref. [7] or employed approximations of the mean-field type [3,8].

When several WGM resonators are placed in the proximity of one another, they become optically coupled due to overlapping evanescent tails of their respective modes. The resulting collective optical excitations in linear regime have been observed experimentally in coupled microspheres and microdisks [9–11] and described theoretically within the framework of *ab initio* approaches [11–14]. At the same time, the nonlinear optics of coupled microresonators is still in its infancy. While lately there was a significant uptick in theoretical attention to this field [15–18], no experiments in this area have yet been reported. This rise of interest to optically coupled resonators is fueled by expectations that these systems would allow for a convenient experimental studies by optical means of some important nonlinear effects of generic nature. In this work we demonstrate theoretically that coupled microdisk resonators with instantaneous Kerr nonlinearity is a convenient system in which such nonlinear effects as Josephson oscillations and self-trapping can be demonstrated. This system is significantly simpler for experimental realization than those considered in Refs. [15,17,18], and we expect, therefore, that this work will motivate experimental studies of nonlinear optical properties of microdisks and other coupled WGM resonators.

Unlike previous theoretical works relying on phenomenological models [15–18], we use an *ab initio* approach to derive equations describing nonlinear dynamics of collective WGM excitations in this system. We show that under certain conditions these equations can be presented in the form of a modified discrete nonlinear Schrödinger equation (DNLSE). The DNLSE is a prominent model known to describe successfully the dynamics of systems as diverse as Bose-Einstein condensates (BECs) in optical lattices, polarons, optical fibers, and biological molecules [17–26]. The DNLSE describes such nonlinear phenomena as self-trapping, discrete breathers, etc., and demonstrate anomalously slow relaxation dynamics [27] (due to boundary losses) similar to the one that appeared in glass materials. This relaxation dynamics has generated recently a great deal of theoretical interest in the context of cold atoms [28–31] and coupled cavities [17,18]. At the same time, while self-trapping in systems with conserving the number of particles or energy has been observed experimentally [24], it is yet to be observed in any physical realization of the DNLSE with losses.

In this work, we demonstrate that the system of coupled microdisk cavities provides a convenient platform for studying nonlinear dynamics in the presence of relaxation. While radiative losses in such a structure are intrinsic to each disk, one can introduce an imbalance of the losses required for anomalous relaxation by coupling one of the disks to a tapered fiber. Such an arrangement, which is usually used to excite WGMs, is known to reduce the Q factor of the fiber-coupled resonator [32] providing thereby a faster relaxation channel through the boundary of the structure. We demonstrate that at certain threshold values of initial conditions and nonlinearity the dynamics of the system exhibits a transition between nonlinear Josephson-like oscillations of light intensity between the disks and a self-trapping behavior. We also show that the transition between these two regimes is manifested in different kinetics of radiative losses in Josephson and self-trapping regimes.

II. *Ab initio* DYNAMICAL EQUATIONS

While we focus in this paper on a nonlinear dynamic of two laterally coupled microdisk resonators, the general dynamic equations can be derived for a more general case of N disks, provided they all lie in the same plane, which is parallel to their surfaces. In the spectral region of high-Q WGM resonances electromagnetic field of a single disk can be described by a simplified two-dimensional model [33], in which its electric [for transverse magnetic (TM) modes] or magnetic [for transverse electric (TE) modes] field is perpendicular to the disk's surface

and is, therefore, characterized by a single function $F^{(i)}(\mathbf{r},t)$. In this approximation, the disks' refractive index is replaced by an effective parameter, n_d, determined from a self-consistency condition [33]. A two-dimensional approximation was also used to describe electromagnetic field of the planar system of several disks (optical molecules) using coupled integral equations [34,35] as well as a modal expansion approach [11]. While the formulation in terms of integral equations is convenient for numerical simulations of planar structures, especially with noncircular elements, the modal expansion is more appropriate for developing an *ab initio* theoretical description of nonlinear effects in WGM resonators.

A. Single disk in presence of external incident field and internal polarization

Before developing the theory of the nonlinear dynamics of WGMs in multiple disks, one has to consider the case of a single disk. We assume that the nonlinearity does not couple TM and TE polarizations and limit our consideration to the TM case. This assumption is valid for disks made of materials with small optical anisotropy and in the absence of wave mixing processes. In the spectral domain the two-dimensional wave equation for the Fourier transformed electric field can be written as

$$\begin{aligned} \nabla^2 F(r,\phi,\omega) + \frac{n_d^2\omega^2}{c^2} F(r,\phi,\omega) &= -\frac{4\pi\omega^2}{c^2} P, \quad r < R, \\ \nabla^2 F(r,\phi,\omega) + \frac{\omega^2}{c^2} F(r,\phi,\omega) &= 0, \quad r > R, \end{aligned} \tag{1}$$

where r and ϕ are, respectively, radial and angular polar coordinates, defined in a coordinate system with the origin at the disk's center, ω is a spectral parameter, not yet identified with any physical frequency, n_d is the effective refractive index of the disk, c is vacuum speed of light, and P is the nonlinear polarization. Usually, Eq. (1) is solved in the context of the scattering problem, when the boundary conditions are of inhomogeneous type defined in the presence of an external "incident" field. At the same time, nonlinear effects are usually described in terms of dynamics of "modal amplitudes," with modes being solutions of a linear problem with homogeneous (no incident field) boundary conditions. The difficulty for the nonlinear theory of WGMs, which are usually excited by an incident field, is consists in necessity to reconcile these two different types of problem. In order to achieve this we, following Ref. [36], introduce a Green's function defined by equations

$$\begin{aligned} \nabla^2 G(\mathbf{r}-\mathbf{r}') + \frac{n_d^2\omega^2}{c^2} G(\mathbf{r}-\mathbf{r}') &= -\delta(\mathbf{r}-\mathbf{r}'), \quad r < R, \\ \nabla^2 G(\mathbf{r}-\mathbf{r}') + \frac{\omega^2}{c^2} G(\mathbf{r}-\mathbf{r}') &= -\delta(\mathbf{r}-\mathbf{r}'), \quad r > R \end{aligned} \tag{2}$$

and boundary conditions

$$\begin{aligned} G(R-0,r') &= G(R+0,r'), \\ \left.\frac{\partial G(r,r')}{\partial r}\right|_{r=R-0} &= \left.\frac{\partial G(r,r')}{\partial r}\right|_{r=R+0}, \\ \left.\frac{\partial \ln[r^{1/2}G(r,r')]}{\partial r}\right|_{r\to\infty} &= i\frac{\omega}{c}, \end{aligned} \tag{3}$$

where the last of these expressions establishes the outgoing field condition at infinity. Using Green's theorem [36] one can express the field in the interior of the disk in terms of the Green's function defined in Eq. (2) and boundary values of the field and its derivative:

$$\begin{aligned} F_m(r) = {} & \frac{8\pi^2\omega^2}{c^2}\int_0^R G_m(r',r)P_m(r')r'dr' \\ & - 2\pi R\left[F_m(R)\frac{\partial G_m(r',r)}{\partial r'} - G_m(R,r)\frac{\partial F_m(r')}{\partial r'}\right]_{r'=R}, \end{aligned} \tag{4}$$

where all quantities with subindex m are angular Fourier coefficients of their respective functions: $\langle\cdot\rangle_m = (1/2\pi)\int_0^{2\pi}\langle\cdot\rangle(\phi)\exp[im\phi]d\phi$. The values of the field and its derivative at the boundary of the disk, $r = R$, are defined via Maxwell boundary conditions demanding continuity of F and its derivative with respect to the radial variable. In the presence of the incident field, $F_{\rm inc}(r,\phi)$, the field outside of the disk is $F_{\rm inc}(r,\phi) + F_{sc}(r,\phi)$, where $F_{sc}(r,\phi)$ is the field scattered by the disk. Taking into account standard conditions for the incident field to be finite at $r = 0$ and for the scattered field to be outgoing at infinity, these fields can be presented as linear combinations of the first-order Bessel (J_m) and Hankel (H_m) functions,

$$F_{\rm inc} = \sum_m a_m J_m(kr)\exp(im\phi), \tag{5}$$

$$F_{sc} = \sum_m b_m H_m(kr)\exp(im\phi), \tag{6}$$

where $k = \omega/c$. Combining Eq. (4) with the boundary conditions, as well as with Eqs. (5) and (6), one arrives at the following expression for the internal ($r < R$) field of the disk:

$$\begin{aligned} F_m(\rho) = {} & 8\pi^2 x^2\int_0^1 G_m(\rho',\rho)P_m(\rho')\rho'd\rho' \\ & - \frac{2i}{\pi x\xi_m(x)}a_m J_m(n_d x\rho), \end{aligned} \tag{7}$$

where we introduced dimensionless spectral parameter $x = kR$ and radial coordinate $\rho = r/R$. Function $\xi_m(x)$ in the second term of Eq. (7) is defined as

$$\xi_m(x) = n_d H_m(x)J_m'(n_d x) - J_m(n_d x)H_m'(x), \tag{8}$$

where $f'(z) \equiv df/dz$.

In the absence of the polarization source, Eq. (7) reproduces a standard solution for the internal field in the linear single disk scattering problem. The scattered field in this case is also found in a standard form,

$$b_m = \alpha_m a_m, \tag{9}$$

where α_m is a linear scattering amplitude defined as

$$\alpha_m = \frac{p_m(x)}{\xi_m(x)}, \tag{10}$$

where $p_m(x)$ is

$$p_m(x) = J_m'(x)J_m(n_d x) - n_d J_m'(n_d x)J_m(x). \tag{11}$$

The poles of $\alpha_m(x)$, which we designate as $x_{m,s}^{(r)} - i\gamma_{m,s}^{(r)}$, are given by complex-valued solutions of equation $\xi(x) = 0$ and

define spectral positions, $x_{m,s}^{(r)}$, and widths, $\gamma_{m,s}^{(r)}$, of linear WGM resonances in a single disk. The subindex s here distinguishes resonances with different radial distributions of the respective internal fields: The value of this index determines the number of maxima of the field in the radial direction. The scattering amplitude has an important property, $\alpha_m(x_{m,s}^{(r)}) \equiv -1$, which results in the following single-pole approximation valid in the vicinity of a selected resonance:

$$\alpha_m = -\frac{i\gamma_{m,s}^{(r)}}{x - x_{m,s}^{(r)} + i\gamma_{m,s}^{(r)}}. \tag{12}$$

Equations (9) and (10) solve the linear scattering problem and describe resonant response of the disk to the external excitation. However, complex frequencies $x_{m,s}^{(r)}$ are not eigenfrequencies of the disk, and their respective field distributions are not its eigenfunctions. In order to define true normal modes of the system together with their eigenvalues, one has to solve the wave equation with boundary conditions formulated in the absence of the incident field (homogeneous boundary conditions). The open nature of the optical resonators makes this problem nontrivial. Several different approaches have been developed to introduce a system of functions, generalizing the concept of modes, that could be used as a basis to describe open systems (see, for instance, recent review [37]). For our goals, the most convenient is the approach based on so-called constant flux modes, reintroduced in the optical context in Ref. [38] and used recently in Ref. [39]. These functions are defined as solutions of the following equations:

$$\begin{aligned} \nabla^2\psi_{m,s}(\rho,\phi) + n_d^2 x_{m,s}^2 \psi_{m,s}(r,\phi) = 0, \quad r < R, \\ \nabla^2\psi_{m,s}(r,\phi) + x^2\psi_{m,s}(r,\phi) = 0, \quad r > R, \end{aligned} \tag{13}$$

with the same boundary conditions as those introduced in Eq. (3) for the Green's function. It is crucial that outside of the disk these functions obey the wave equation with generic spectral parameter x rather than with the eigenvalue $x_{m,s}$. Only functions defined this way form, in combination with their adjoint counterparts, a complete biorthogonal set with an inner product and norm defined over the *interior* of the disk:

$$\int_0^1 \psi_{m,s}(\rho)[\overline{\psi}_{l,p}(\rho)]^*\rho d\rho = N_{m,s}^2\delta_{m,l}\delta p,s. \tag{14}$$

Adjoint functions $\overline{\psi}_{l,p}(\rho)$ appearing in Eq. (14) are solutions of equations

$$\begin{aligned} \nabla^2\overline{\psi}_{m,s}(\rho,\phi) + n_d^2\left[x_{m,s}^2\right]^*\overline{\psi}_{m,s}(r,\phi) = 0, \quad r < R, \\ \nabla^2\overline{\psi}_{m,s}(r,\phi) + x^2\overline{\psi}_{m,s}(r,\phi) = 0,1, \quad r > R, \end{aligned} \tag{15}$$

with incoming boundary conditions at infinity. The eigenvalues $x_{m,s}$ are defined by equation

$$n_d x_{m,s} H_m(x) J_m'(n_d x_{m,s}) - x J_m(n_d x_{m,s}) H_m'(x) = 0 \tag{16}$$

and are complex-valued functions of the spectral parameter x, which becomes an integration variable upon transformation of the fields back to the time domain.

Since eigenfunctions $\psi_{m,s}$ obey the same boundary conditions as the Green's function, $G_m(\rho,\rho')$, they can be used to generate its spectral expansion,

$$G_m(\rho,\rho') = -\frac{R^2}{2\pi n_d^2}\sum_s \frac{\psi_{m,s}(x_{m,s}n_d\rho)\overline{\psi}_{m,s}^*(x_{m,s}n_d\rho')}{x^2 - x_{m,s}^2}. \tag{17}$$

The same set of functions can be used to present the internal field of the disk

$$F_m(\rho,x) = \sum_s D_{m,s}(x)\psi_{m,s}(x_{m,s}n_d\rho), \tag{18}$$

yielding, in combination with Eqs. (4) and (17), and biorthogonality relation [Eq. (14)], the following system of equations for modal amplitudes $D_{m,s}$:

$$D_{m,s}\left(x^2 - x_{m,s}^2\right) = -\frac{4\pi x^2}{n_d^2}P_{m,s}(x) - \kappa_{m,s}a_m\frac{A_{m,s}(x)}{p_m(x)}. \tag{19}$$

Here we introduced projections of the nonlinear polarization, $P_{m,s}$, and incident field, $A_{m,s}$, onto eigenfunctions of the disk:

$$P_{m,s}(x) = \int_0^1 P_m(x,\rho)\overline{\psi}_{m,s}^*(x_{m,s}n_d\rho)\rho d\rho, \tag{20}$$

$$A_{m,s}(x) = \frac{2}{\pi x}\int_0^1 J_m(n_d x\rho)\overline{\psi}_{m,s}^*(x_{m,s}n_d\rho)\rho d\rho, \tag{21}$$

and a parameter $\kappa_{m,s}$ defined as

$$\kappa_{m,s} \equiv \alpha_m(x)\left(x^2 - x_{m,s}^2\right). \tag{22}$$

Parameter $\kappa_{m,s}$ in the last term of Eq. (19) characterizes the efficiency of coupling of the incident radiation to the internal modes of the disk. The structure of this parameter, which we call external coupling parameter, reflects the distinction between external and internal excitation mechanisms: **External** incident field induces response at scattering resonances, while **internal** excitation (polarization term) generates response at the eigenfrequencies. Taking into account Eq. (12) one can present $\kappa_{m,s}$ in vicinity of $x_{m,s}$ as

$$\kappa \approx -\frac{2i\gamma_{m,s}x_{m,s}(x - x_{m,s})}{x - x_{m,s}^{(r)} + i\gamma_{m,s}^{(r)}}. \tag{23}$$

For resonances with low Q factors the difference between eigenfrequencies and scattering resonances can be quite significant, resulting in a strong frequency dependence of the coupling to the external field. However, for high-Q resonances, numerical calculations indicate (see also Ref. [38]) that $\mathrm{Re}[x_{m,s}] - x_{m,s}^{(r)}$, as well as $\mathrm{Im}[x_{m,s}] - \gamma_{m,s}^{(r)}$ are much smaller than the individual imaginary parts of these quantities. In this case κ can be simplified to the following form:

$$\kappa \approx -2i\gamma_{m,s}x_{m,s}, \tag{24}$$

which shows that efficiency of coupling to the modes of the disk from outside is proportional to the width of these modes. This physically clear result expresses the fact that one cannot couple from outside to a completely closed system. Here this

result is derived within an *ab initio* approach, while in many other cases (see for instance, Ref. [40]) a similar factor is introduced into the respective term "by hand."

B. Nonlinear dynamics of multiple optically coupled disks in the frequency domain

1. General equations

The case of multiple disks can be treated by applying Eq. (19) to each disk of the structure and including in the term containing the incident field contributions from the fields scattered by all other disks [11]:

$$a_m \to a_m^p + \sum_{v\neq p}\sum_n b_n^v t_{m-n}^{v,p}. \tag{25}$$

Here indexes p,v enumerate disks comprising the structure, and $t_{m-n}^{v,p} = e^{(n-m)\theta_{v,p}} H_{m-n}(xR_{v,p}/R)$ describes optical coupling between the disks, where $R_{v,p}$ and $\theta_{v,p}$ are, respectively, radial and angular polar coordinates of vth disk relative to the pth one. This terms arises from transformation of the field scattered by the vth disk to the coordinate system centered at the pth disk using Graf's addition theorem for Hankel functions [41]. If all the disks are arranged along a single line, which is chosen as a polar axis of the coordinate system, one has $\theta_{pv} = \pi$ for $p < v$ and $\theta_{pv} = 0$ for $p > v$.

Equation (19) in the multiple disk case must be complimented by an equation relating scattering coefficients b_n^p of different disks to each other. In the absence of nonlinearity this equation is again obtained by substituting Eq. (25) to the single disk Eq. (9), which gives [11]

$$b_m^p = \alpha_m(x)\left[a_m^p + \sum_n\sum_{v\neq p} t_{m-n}^{v,p} b_n^v\right]. \tag{26}$$

While the presence of nonlinear polarization in Eq. (1) modifies Eq. (26), this modification can be neglected since it is proportional to two relatively weak effects: interdisk coupling and single-disk nonlinearity. Only when frequency shifts due to any of these effects becomes comparable with linear frequencies of the resonator, nonlinear corrections to Eq. (26) should be taken into account. Combining Eq. (19) with Eqs. (25) and (26), one can eliminate coefficients of the scattered field, b_p^m, from the equation for the modal amplitudes and obtain the closed equation for the latter:

$$\left(x^2 - x_{m,s}^2\right)\tilde{D}_{m,s}^p - \kappa_{m,s}(x)\sum_n\sum_{v\neq p} t_{m-n}^{v,p}\tilde{D}_{n,s}^v(x)$$
$$= -i\kappa_{m,s}(x)a_m^p - \frac{4\pi x^2 p_m}{n_d^2 A_{m,s}}\tilde{P}_{m,s}^p, \tag{27}$$

where we introduced renormalized modal amplitude $\tilde{D}_{m,s}^p$ related to the original amplitude defined in Eq. (18) according to

$$\tilde{D}_{m,s}^p \equiv \frac{p_m}{A_{m,s}} D_{m,s}^p. \tag{28}$$

This amplitude describes the field outside of the resonator produced by an internal mode with amplitude $D_{m,s}^p$. It is important to note that the external coupling coefficient $\kappa_{m,s}$ appears in Eq. (27) not only in the term containing incident field, but also in the one describing interdisk coupling. This is a reflection of the obvious, but still not always appreciated, fact that the optical coupling between disks occurs via scattered rather than internal fields.

Equation (27) must be, of course, complimented by an expression for the nonlinear polarization in terms of modal amplitudes, $\tilde{D}_{m,s}$. Assuming nonlinearity of Kerr type, we can present nonlinear polarization term $P(\omega)$ as

$$P(\mathbf{r},x) = \frac{cn_d^2 n_2}{16\pi^2}\int \frac{dx_1}{2\pi}\frac{dx_2}{2\pi} F(\mathbf{r},\tilde{x}_{1,2})F(\mathbf{r},x_1)F^*(\mathbf{r},x_2), \tag{29}$$

where $\tilde{x}_{1,2} \equiv x - x_1 + x_2$ and we used approach of Ref. [42] to express Kerr nonlinear polarization in terms of standard nonlinear refractive index n_2. Combining Eq. (29) with modal expansion Eq. (18) one can finally derive the following expression for the component of the nonlinear polarization $\tilde{P}_{m,s}$ in terms of modal amplitudes $D_{m,s}(x)$:

$$\tilde{P}_{m,s}(x) = \sum_{\nu_1,\nu_2,\nu_3}\delta_{m-m_2+m_3,m_1}\Lambda_{\nu_1,\nu_2,\nu_3}^{m,s}\int\frac{dx_1}{2\pi}\frac{dx_2}{2\pi}D_{\nu_1}(\tilde{x}_{1,2})$$
$$\times D_{\nu_2}(x_1)D_{\nu_3}^*(x_2), \tag{30}$$

where for brevity we combined double indexes m_i,s_i in single indexes ν_i, and introduced nonlinear intermode coupling coefficients $\Lambda_{\nu_1,\nu_2,\nu_3}^{m,s}$ defined as

$$\Lambda_{\nu_1,\nu_2,\nu_3}^{m,s} = \frac{cn_d^2 n_2}{16\pi^2}\int_0^1 d\rho\rho\psi_{\nu_1}(x_{\nu_1}n_d\rho)\psi_{\nu_2}(x_{\nu_2}n_d\rho)\psi_{\nu_3}(x_{\nu_3}n_d\rho)$$
$$\times\overline{\psi}_{m,s}^*(x_{m,s}n_d\rho). \tag{31}$$

The derived equations (27)–(31) provide an *ab initio* foundation for studying a variety of nonlinear processes in the the system of coupled disk resonators with Kerr nonlinearity. The next step in development of the theory would include Fourier transformation of the derived equations back to time domain. This procedure cannot be carried out exactly and requires approximations of a "slow changing amplitude" type. The implementation of the latter, however, depends on the type of nonlinear processes being studied. In this paper we are interested in self-trapping dynamics in the system of coupled disks, thus in the subsequent sections of the paper we apply Eqs. (27)–(31) to this particular problem.

2. Dynamic of modal amplitudes in a double-disk optical "molecule"

In what follows we limit our consideration to the case of only two disks, which we study in the so-called resonant approximation [11]. This approximation implies that we only take into account coupling between degenerate phase-matched modes of the disks. These are clockwise and counterclockwise modes characterized by azimuthal numbers of opposite signs. The phase matching means that mode with $m = M$ in disk 1 couples only to the mode $m = -M$ of disk 2 and vice versa. On a formal level this is justified by inequality $t_{2M} \gg t_0$ valid

for $M \gg 1$. In this approximation Eq. (27) takes the following form:

$$\begin{aligned}
\left(x^2 - x_M^2\right)\tilde{D}_M^1 - \kappa_{m,s}(x)t_{2M}^{1,2}\tilde{D}_{-M}^2(x) &= -\frac{4\pi x^2 p_M}{n_d^2 A_M}\tilde{P}_M^1,\\
\left(x^2 - x_M^2\right)\tilde{D}_M^2 - \kappa_{m,s}(x)t_{2M}^{1,2}\tilde{D}_{-M}^1(x) &= -\frac{4\pi x^2 p_M}{n_d^2 A_M}\tilde{P}_M^2,\\
\left(x^2 - x_M^2\right)\tilde{D}_{-M}^1 - \kappa_{m,s}(x)t_{2M}^{1,2}\tilde{D}_M^2(x) &= -\frac{4\pi x^2 p_M}{n_d^2 A_M}\tilde{P}_{-M}^1,\\
\left(x^2 - x_M^2\right)\tilde{D}_{-M}^2 - \kappa_{m,s}(x)t_{2M}^{1,2}\tilde{D}_M^1(x) &= -\frac{4\pi x^2 p_M}{n_d^2 A_M}\tilde{P}_{-M}^2,
\end{aligned} \tag{32}$$

where we abridged notations by replacing double index m,s with a single index M having in mind that in the resonant approximation all involved modes have the same radial index set to be equal to unity. In Eq. (32) we also omitted the term with the incident field since we model excitations of the dynamics in this paper by initial conditions rather than by an external field.

Transformation of Eq. (32) to the time domain is based on a slow amplitude approximation, when the nonlinear dynamics is presented as a slow modulation of fast linear oscillations of the field:

$$\tilde{D}_M^p(t) = \tfrac{1}{2}\left[S_M^p(t)e^{-ix_0 t} + \text{c.c.}\right], \tag{33}$$

where S_M^p is a slow changing amplitude, x_0 is the frequency of the linear dynamics, and c.c. means "complex conjugated" term. In the spectral domain this approximation has the following form:

$$\tilde{D}_M^p(x) = \tfrac{1}{2}\left\{S_M^p(x)\delta(x - x_0) + \left[S_M^p(x)\right]^*\delta(x + x_0)\right\}. \tag{34}$$

The choice of x_0 depends on the problem at hand. For instance, in the presence of an external incident field, x_0 would be set by its frequency, while in the case of initial value problem, considered in this work, the linear dynamics is determined by the poles of the Green's function [Eq. (17)]. These poles are solutions of equation $x_{m,s}(x) = x$, and it is clear from Eqs. (8) and (16) that they coincide with the scattering resonances. Thus, in this case $x_0 = \text{Re}[x_M^{(r)}]$ and Eq. (24) for the external coupling parameter becomes exact.

When using Eq. (34) to convert system (32) to the time domain, one needs to take into account the dependence of the eigenfrequencies on the spectral parameter x and expand it in the power series around $x = x_0$. In the slow amplitude approximation one only keeps the term linear in x, which corresponds to the first-order time derivative in the time-domain:

$$x_M(x) \approx x_0 + (x - x_0)\left.\frac{dx_M}{dx}\right|_{x=x_0}.$$

While the dx_M/dx term affects the coefficient in front of term with the first-order time derivative of the modal amplitude, its numerical estimates showed that in the case under consideration in this work it can be neglected.

Time-domain expression for the nonlinear polarization terms is obtained by Fourier-transforming Eq. (30) with the help of Eq. (34) and restricting summation over modes only to those with $s = 1$ and $m = \pm M$. In doing so, we also neglect all fast oscillating terms at combination frequencies. Combining the result with the Fourier transform of the linear part of Eq. (32) we obtain the final set of time-dependent equations for modal amplitudes

$$\begin{aligned}
i\frac{dS_{\pm M}^{(v)}(\tau)}{d\tau} + i\gamma_M S_{\pm M}^{(v)}(\tau) + h_M S_{\mp M}^{(p)}(\tau)\\
= -\zeta\Gamma_M S_{\pm M}^{(v)}\left[\left|S_{\pm M}^{(v)}\right|^2 + 2\left|S_{\mp M}^{(v)}\right|^2\right].
\end{aligned} \tag{35}$$

In these equations we introduced dimensionless time $\tau = tc/R$ and linear coupling coefficient $h_M = i\gamma_M^{(r)}t_{2M}^{(12)}$ (recall that the imaginary part of Hankel function entering $t_{2M}^{(12)}$ is much larger than its real part for $M \gg 1$, so that h_M has very small imaginary part). Kerr nonlinearity results in self-coupling of modes and cross-coupling between counterpropagating modes. The strength of nonlinear interactions is characterized by material parameter $\zeta = (cn_2x_0)/(4\pi)$ and the dimensionless resonator enhancement parameter

$$\Gamma_M = x_0 R^2 |A_M/p_M|^2 \int_0^1 \left[\psi\left(x_M^{(r)}n_d\rho\right)\right]^2\left|\psi\left(x_M^{(r)}n_d\rho\right)\right|^2\rho d\rho. \tag{36}$$

Both parameters h_M and Γ_M are, in general, complex-valued, but for high-Q modes their imaginary parts are much smaller than γ_M, which describes the main contribution to the radiative losses of our systems. Therefore, below we assume that $\text{Im}(h_M) = \text{Im}(\Gamma_M) = 0$. The resulting equations give a complete *ab initio* description of the nonlinear dynamics of coupled disks in the resonant approximation. A resonator-induced enhancement of nonlinear effects manifests itself through parameter Γ_m, which is found to increase by six orders of magnitude when the azimuthal number m changes from $m = 5$ to $m = 40$ (see Fig. 1). This enhancement reflects

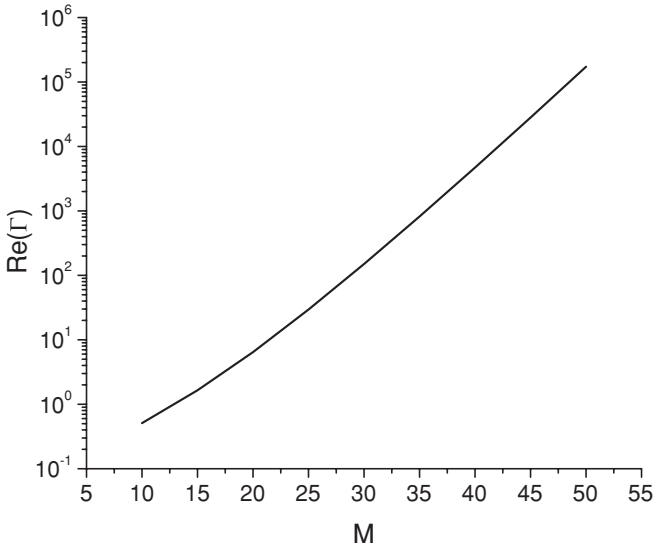

FIG. 1. Nonlinear cavity enhancement factor showing significant increase over the range of m.

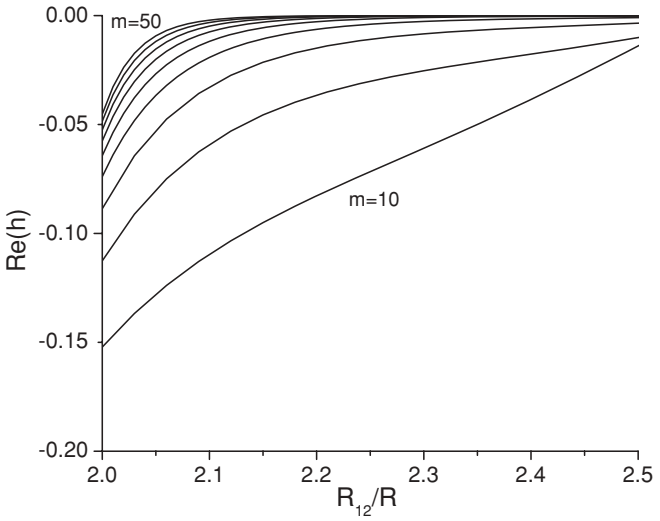

FIG. 2. Linear interdisk coupling coefficient for values of m ranging from $m = 10$ (lower line) to $m = 50$ (upper line).

drastic concentration of the field of the WGM modes within its effective volume. Figure 2 shows the linear interdisk coupling parameter as a function of the interdisk distance for values of the mode order m ranging from $m = 10$ to $m = 50$. It is interesting that, while the nonlinear parameter shows fast growth with m, the linear interdisk coupling actually decreases with m while also becoming more short ranged. This is explained by the fact that this parameter is a product of two factors: the Hankel function, which grows very fast with m, and the radiative decay rate $\gamma_M^{(r)}$, which significantly diminishes with m. The result presented in this plot shows the interplay of these two opposite tendencies.

III. SELF-TRAPPING TRANSITION IN THE DOUBLE DISK SYSTEM

Nonlinear discrete systems exhibit a transition from a Josephson-like oscillatory motion to a self-trapping behavior when the nonlinearity strength increases beyond some critical value. The phenomenon has been studied extensively for a variety of systems ranging from coupled nonlinear waveguides to BECs in optical lattices and biological systems [17–26], while recently it has been also observed experimentally in the frame of BECs [24]. Here we show that coupled optical microdisks can be used as a prototype system to analyze and observe experimentally such phase transition.

Our analysis of the temporal behavior of the electric field relies on Eq. (35), where (to the first approximation) we neglect radiative losses ($\gamma_0 = 0$). An analytical treatment of the dynamics can be achieved if we rewrite Eq. (35) in terms of the Stokes parameters defined as

$$\begin{aligned} J_\pm^0 &= \left|S_{\pm1}^{(1)}\right|^2 + \left|S_{\mp1}^{(2)}\right|^2, \\ J_\pm^{(x)} &= \left(S_{\pm1}^{(1)}\right)^* S_{\mp1}^{(2)} + S_{\pm1}^{(1)}\left(S_{\mp1}^{(2)}\right)^*, \\ J_\pm^{(y)} &= i\left[S_{\pm1}^{(1)}\left(S_{\mp1}^{(2)}\right)^* - \left(S_{\pm1}^{(1)}\right)^* S_{\mp1}^{(2)}\right], \\ J_\pm^{(z)} &= \left|S_{\pm1}^{(1)}\right|^2 - \left|S_{\mp1}^{(2)}\right|^2. \end{aligned} \tag{37}$$

The first of these parameters, $J_\pm^0$, is associated with the total field intensity distributed between the coupled counterclockwise (clockwise) and clockwise (counterclockwise) modes of disks 1 and 2, respectively. One can show that $dJ_\pm^{(0)}/d\tau = 0$; that is, $J_\pm^0$ is a conserved quantity. Of special interest is the $J_\pm^{(z)}$ component which describes the intensity imbalance between counterclockwise (clockwise) and clockwise (counterclockwise) modes of disks 1 and 2. Using the Stokes variables Eq. (37), we can rewrite Eqs. (35) in the following form:

$$\frac{d\mathbf{J}_\pm}{d\tau} = \mathbf{J}_\pm \times \mathbf{B}, \tag{38}$$

where we introduced the Stokes vector $\mathbf{J}_\pm \equiv (J_\pm^{(x)}, J_\pm^{(y)}, J_\pm^{(z)})$, the pseudomagnetic field $\mathbf{B} \equiv (2,0,\chi J_\pm^{(z)} + 2\chi J_\mp^{(z)})$ with $\chi = \zeta\Gamma_M/h_M$ and redefined the time variable as $\tau \to \tau/h_M$.

For the intensity imbalance between the disks $J_\pm^{(z)}$, one can derive the following equation:

$$\frac{d^2 J_\pm^{(z)}}{d\tau^2} + 4J_\pm^{(z)} - 2\chi J_\pm^{(x)}(J_\pm^{(z)} + 2J_\mp^{(z)}) = 0. \tag{39}$$

Direct integration of Eq. (39) for various initial conditions indicates that there is always a critical value χ_{cr} of the nonlinearity, for which $J_\pm^{(z)}$ shows a transition from a regime where it is always positive or negative to a regime that oscillates around zero. An example of such behavior is shown in Figs. 3(a) and 3(b). The former case is associated to the self-trapping regime, while the latter one is associated with the nonlinear Josephson-like oscillations [17,21–24]. Obviously, the critical value of the nonlinearity χ_{cr} above which energy transfer from one disk to another can take place depends on the initial preparation of the field excitation in the coupled microdisk system.

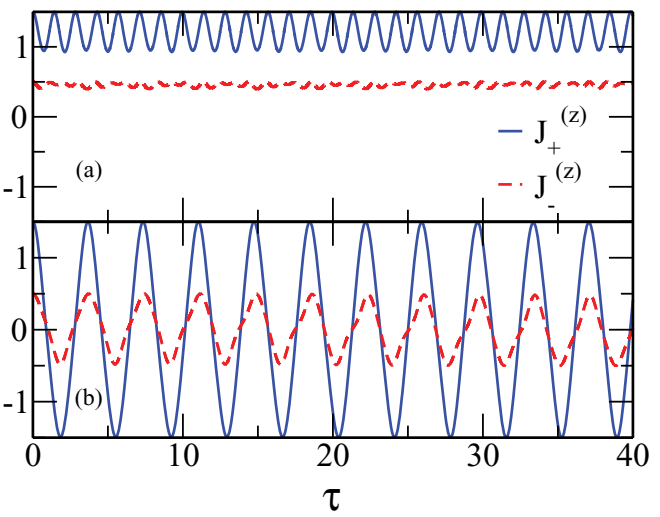

FIG. 3. (Color online) Imbalance intensity $J_\pm^{(z)}(\tau)$ for the two-disks system. We have used some generic initial conditions such that $|S_+^{(1)}|^2 = 1.5$, $|S_-^{(1)}|^2 = 0.5$, $|S_+^{(2)}|^2 = |S_-^{(2)}|^2 = 0$. Plot (a) is obtained with $\chi = 2$ (self-trapping regime), while plot (b) corresponds to $\chi = 1$ (Josephson oscillation regime). The solid and dashed lines correspond to $J_\pm^{(z)}$ components, respectively.

The smallest value of χ_{cr} is realized for initial conditions, $J_{\pm}^{(z)}(0) = 1$ with the norm $J_{\pm}^{0}(0) = 1$. These correspond to an initial excitation of the clockwise and counterclockwise modes of one of the disks. From Eq. (38) we find that

$$J_{+}^{(x)} + J_{-}^{(x)} = -\frac{\chi}{4}[(J_{+}^{(z)} + J_{-}^{(z)})^2 + 2J_{+}^{(z)}J_{-}^{(z)}] + \frac{3\chi}{2}. \quad (40)$$

Substituting the first term on the right-hand side of Eq. (40), from Eq. (39), and using the fact that $J_{+}^{(z)}$ and $J_{-}^{(z)}$ are symmetric, we eventually get

$$\frac{d^2 J_{+}^{(z)}}{d\tau^2} + \left(4 - \frac{9\chi^2}{2}\right) J_{+}^{(z)} + \frac{9\chi^2}{2} J_{+}^{(z)3} = 0. \quad (41)$$

Equation (41) admits the following solution:

$$J_{\pm}^{(z)}(\tau) = \begin{cases} \mathrm{cn}(2\tau;\eta); & \eta < 1, \\ \mathrm{dn}(3\chi\tau/2;\eta^{-1}); & \eta > 1, \end{cases} \quad (42)$$

where $\mathrm{cn}(u,\eta)$ and $\mathrm{dn}(u,\eta)$ are Jacobian elliptic functions, and $\eta = 3\chi/4$ is the modulus of the elliptic function. The value $\eta = 1$, corresponding to $\chi_{cr} = 4/3$, marks a transition from an oscillatory to a self-trapped behavior.

While the previous theoretical analysis allows us to calculate quantitatively the solutions of Eq. (38) and derive an expression for the critical nonlinearity strength, we find it useful to provide also a qualitative argument explaining the existence of Josephson to self-trapping transition. The main observation is based on the fact that an initial preparation will be redistributed in a way that it will minimize the Hamiltonian function (energy) associated with our system. The latter can be derived from the equations of motion (35) and has the form

$$\mathcal{H} = \sum_i \Big[(S_{-}^{i-1} + S_{-}^{i+1}) S_{+}^{i\,*} + (S_{+}^{i-1} + S_{+}^{i+1}) S_{-}^{i\,*} + \frac{\chi}{2}(|S_{+}^{i}|^4 + |S_{-}^{i}|^4) + 2\chi(|S_{+}^{i}|^2 |S_{-}^{i}|^2) \Big], \quad (43)$$

In the self-trapping regime, the energy is concentrated at the specifics modes which are initially populated (initial field distribution). For such field configuration we get $\mathcal{H}_{ST} = 3\chi$. On the other hand, in the limit of Josephson oscillations the energy is distributed (on the average) uniformly over the whole system. If one assumes that $S_{\pm}^{(i)} \propto 1/\sqrt{2}$, we get the corresponding value of the energy function $\mathcal{H}_{JO} = (3\chi + 4)/2$. The critical nonlinearity χ_{cr} for which the transition from one regime to another occurs can be evaluated by equating the two energy distributions. Our simple argument gives $\chi_{cr} = 4/3$, which coincides with the result obtained from the rigorous solution presented above.

This analysis can be further extended to the case when the counterpropagating modes in each disk are allowed to interact with each other due to, for instance, surface roughness induced scattering [33,43]. This interaction can be described by adding an extra term, $\nu_M S_{\pm}^{(i)}$, to the left side of Eq. (35), where ν_M describes the strength of the intradisk coupling at each disk. Using the same analysis as above, one can estimate the critical value of nonlinearity. For example, for the initial conditions that we have used, $J_{+}^{(z)} = J_{-}^{(z)} = 1$, we find $\chi_{cr} = 4/3$, independently from the value of the intradisk coupling. Again, our numerical calculations agree with the prediction of the heuristic argument.

IV. LEAKING DYNAMICS

A natural question is how the self-trapping phenomenon affects the relaxation dynamics of this system once a leakage is introduced in one of the disks. Experimentally, this can be achieved by coupling one of the disks to a tapered fiber, as discussed in the Introduction. This will result in the imbalance between decay rates of the two disks so that the smaller intrinsic decay rate in the second disk can be neglected. Theoretically, we describe this situation by restoring a radiative decay rate, γ_0, only in the first of the Eq. (35).

The object of interest is the total intensity $P(\tau) = J_{+}^{(0)} + J_{-}^{(0)}$, which is no longer a conserving quantity. In order to eliminate effects due to trivial exponential decay of the intensity, we present the numerical results for the relaxation dynamics in Fig. 4 in terms of the rescaled parameter $\tilde{P} = P\exp(\gamma_0\tau)$. Two different relaxation regimes are observed in the short time limit. While for $\chi \leqslant 4/3$ the rescaled norm oscillates with a period similar to that of the corresponding closed system in the Josephson regime, for $\chi > 4/3$ there is an exponential decay, which is not eliminated by the rescaling procedure. The origin of this discrepancy is associated with the self-trapping phenomenon. Indeed, if initial excitation is created in the leaky disk and $\chi > 4/3$, it becomes trapped and starts leaking out at a faster rate. When, however, the total intensity decreases and the system moves to the Josephson regime the decay process slows down since the light intensity

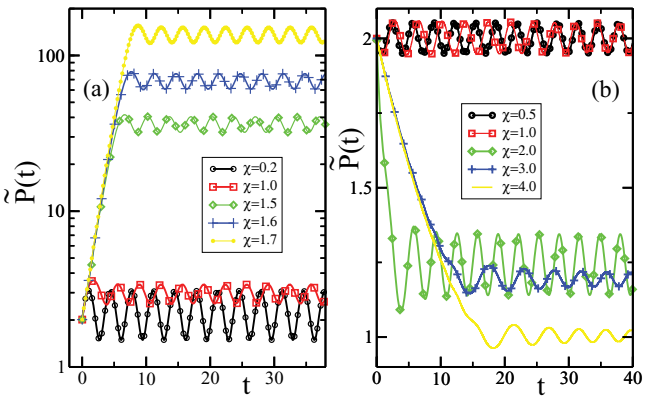

FIG. 4. (Color online) Temporal behavior of the total intensity remaining inside the two disks when the first one is attached to a fiber. Panels (a) and (b) present the rescaled total intensity $\tilde{P}(t)$ for initial excitation at the second disk and at the first disk, respectively. In (a) the leaking constant is $\gamma = 0.7$ while in (b) we have used $\gamma = 0.05$. In both cases, we have used various nonlinearity strengths above and below the critical nonlinearity parameter. (Respective curves are marked by different symbols as indicated in the plots).

oscillates between the leaky and the nonleaky disk. On the other hand, if we excite the nonleaking disk, then for $\chi > 4/3$, the initial decay is slower, which manifests itself in the initial growth of the rescaled intensity $\tilde{P}$.

To achieve a better understanding of the initial decay in the self-trapped regime, we have analyzed the eigenvalue problem associated with Eq. (35) in the presence of the dissipation; that is,

$$\mathcal{E}\Phi_{\pm1}^{(i)} = -i\gamma_0\delta_{1,i}\Phi_{\pm1}^{(i)} - \Phi_{\mp1}^{(j)} - \chi\Phi_{\pm1}^{(i)}\left[\left|\Phi_{\pm1}^{(i)}\right|^2 + 2\left|\Phi_{\mp1}^{(i)}\right|^2\right]. \quad (44)$$

By multiplying each set of the equations in (45) by the corresponding $\Phi_{\pm1}^{(i)*}$, and adding the resulting expressions for the propagating and counter-propagating modes associated with the two disks, we get

$$\mathcal{E} = -\left(\Phi_{+1}^{(i)*}\Phi_{-1}^{(j)} + \Phi_{-1}^{(j)*}\Phi_{+1}^{(i)}\right) - \chi\left(\left|\Phi_{+1}^{(i)}\right|^4 + \left|\Phi_{-1}^{(j)}\right|^4\right) - 2\chi\left(\left|\Phi_{+1}^{(i)}\right|^2\left|\Phi_{-1}^{(i)}\right|^2 + \left|\Phi_{+1}^{(j)}\right|^2\left|\Phi_{-1}^{(j)}\right|^2\right) - i\gamma_0\left|\Phi_{j-i}^{(1)}\right|^2, \quad (45)$$

where we have used the normalization $|\Phi_{+1}^{(i)}|^2 + |\Phi_{-1}^{(j)}|^2 = 1$ for $i \neq j$ and $i,j = 1,2$. Equating real and imaginary parts of both sides of the above equations, we get that $\mathcal{I}m\mathcal{E} = -\gamma_0|\Phi_{+1}^{(1)}|^2 = -\gamma_0|\Phi_{-1}^{(1)}|^2$. Using the last equality together with the normalization condition we can conclude that $|\Phi_{-1}^{(i)}|^2 = |\Phi_{+1}^{(i)}|^2$. Therefore, the four sets of equations in Eq. (45) reduce to the following eigenvalue problem:

$$\mathcal{E}\Phi_{+1}^{(1)} = -i\gamma_0\Phi_{+1}^{(1)} - \Phi_{-1}^{(2)} - 3\chi\left|\Phi_{+1}^{(1)}\right|^2\Phi_{+1}^{(1)},$$
$$\mathcal{E}\Phi_{-1}^{(2)} = -\Phi_{+1}^{(1)} - 3\chi\left|\Phi_{-1}^{(2)}\right|^2\Phi_{-1}^{(2)}, \quad (46)$$

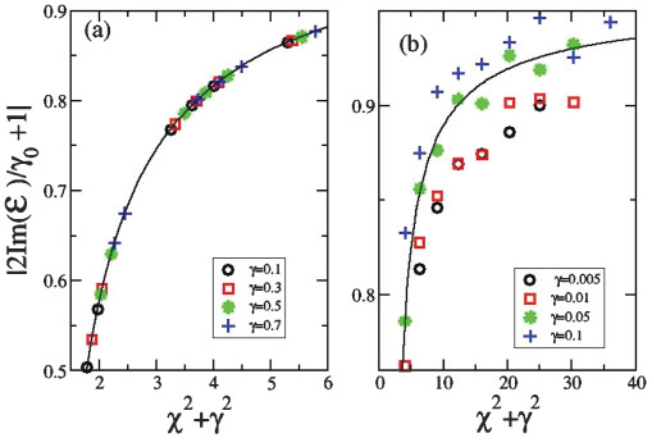

FIG. 5. (Color online) Decay rates extracted from the analysis of the rescaled total intensity shown in Figs. 4(a) and 4(b). Plot (a) corresponds to initial excitation at the second disk. Plot (b) reports the initial decay rates when the excitation is prepared at the first disk. In both cases, we have used various nonlinearity strengths χ and leaking constants γ. The black lines represent the theoretical predictions Eq. (47), while various symbols correspond to different values of nonlinearity.

which can be solve exactly. Specifically, we find that for $\chi < \chi^* \equiv (1/3)\sqrt{4-\gamma_0^2}$ there are two (equidistributed among the disks) leaking modes corresponding to an energy distributed equally between the two disks $|\Phi_{+1}^{(1)}|^2 = |\Phi_{-1}^{(2)}|^2$.[1] The associated complex eigenvalues $\mathcal{E}$ have an imaginary part $\mathrm{Im}(\mathcal{E}) = -\gamma_0/2$, which dictates their decay rate. For $\chi > \chi^*$ two new (nonequidistributed) modes appear with

$$\mathrm{Im}(\mathcal{E}^{(\pm)}) = (\gamma_0/2)\left\{-1 \pm \sqrt{1-(4/3)/\left[\chi^2+\gamma_0^2\right]}\right\}. \quad (47)$$

These solutions correspond to an nonequal energy occupations $|\Phi_{+1}^{(1)}|^2 = \frac{1}{2}\{1 \mp \sqrt{1-(4/3)/[\chi^2+\gamma^2]}\}$. As expected, the $\mathcal{I}m(\mathcal{E}^{(+)})$ $[\mathcal{I}m(\mathcal{E}^{(-)})]$ decay rate corresponds to the mode, which has most of the intensity concentrated in the (non-)leaky disk. These rates are in agreement with those extracted from our simulations (see Fig. 5).

V. CONCLUSION

Using an *ab initio* approach, we derived the equations that describe the dynamics of amplitudes of high-Q WGMs in a system of two evanescently coupled microdisk resonators. Taking into account linear coupling only between counterpropagating modes in adjacent disks, we studied manifestations of self-trapping phenomenon in the relaxation dynamics. It should be noted that similar effect was also discussed in Refs. [17,18] within the framework of quantum electrodynamics. An important distinction between the system studied in this paper and those considered in Refs. [17,18] lies in the mechanism responsible for enhancement of nonlinear effects. In Refs. [17,18] this enhancement was due to resonant interaction of photons with material excitations such as atoms or excitons, while in this work the enhancement occurs due to small volume of WGMs. As a result, the nonlinear effects considered in this paper can be observed at room temperature. For instance, we found that in the presence of the decay rate imbalance between the coupled disks, there exists an anomalous relaxation behavior similar to the one discussed in Refs. [27–31]. This result identifies the system of coupled optical resonators as a convenient platform for experimental study of this phenomenon, which, so far, has eluded experimental observation.

ACKNOWLEDGMENTS

H.R. and T.K. acknowledge financial support by Grant No. FA 9550-10-1-0433 from AFOSR, the DFG Research Unit 760, and by the US-Israel Binational Science Foundation (BSF), Jerusalem, Israel. One of the authors (L.D.) would like to thank Arkadi Chipulin and Thomas Pertsch for their hospitality during L.D.'s stay in Jena, where part of this work was performed.

[1]We note that the difference between critical value of nonlinearity for self-trapping behavior obtained from analysis presented here and that of Sec. III is due to the occupation distribution of the initial excitation.

[1] V. M. Braginsky, M. L. Gorodetsky, and V. S. Ilchenko, Phys. Lett. A **137**, 393 (1989).
[2] H. B. Lin and A. J. Campillo, Phys. Rev. Lett. **73**, 2440 (1994).
[3] D. Braunstein, A. M. Khazanov, G. A. Koganov, and R. Shuker, Phys. Rev. A **53**, 3565 (1996).
[4] S. M. Spillane, T. J. Kippenberg, and K. J. Vahala, Nature (London) **415**, 621 (2002).
[5] A. Savchenkov, A. Matsko, D. Strekalov, M. Mohageg, V. Ilchenko, and L. Maleki, Phys. Rev. Lett. **93**, 243905 (2004).
[6] D. V. Strekalov and N. Yu, Phys. Rev. A **79**, 041805(R) (2009).
[7] A. Matsko, A. Savchenkov, D. Strekalov, V. Ilchenko, and L. Maleki, Phys. Rev. A **71**, 033804 (2005); Demetrios N. Christodoulides and Nikos K. Efremidis, Opt. Lett. **27**, 568 (2002).
[8] A. Fomin, M. Gorodetsky, I. Grudinin, and V. Ilchenko, J. Opt. Soc. Am. B **22**, 459 (2005).
[9] B. M. Moeller, U. Woggon, and M. Artemeyev, Opt. Lett. **30**, 2116 (2005).
[10] Y. Hara, T. Mukaiyama, K. Takeda, and M. Kuwata-Gonokami, Phys. Rev. Lett. **94**, 203905 (2005).
[11] C. Schmidt, A. Chipouline, T. Kaesebier, E. B. Kley, A. Tunnermann, T. Pertsch, V. Shuvayev, and L. I. Deych, Phys. Rev. A **80**, 043841 (2009).
[12] H. Miyazaki and Y. Jimba, Phys. Rev. B **62**, 7976 (2000).
[13] T. M. Benson, S. V. Boriskina, P. Sewell, A. Vukovic, S. C. Greedy, and A. I. Nosich, *Micro-Optical Resonators for Microlasers and Integrated Optoelectronics*, Vol. 216 of Frontiers in Planar Lightwave Circuit Technology, NATO Science Series (Springer, Netherlands, 2006), pp. 39–70.
[14] L. I. Deych and O. Roslyak, Phys. Rev. E **73**, 036606 (2006).
[15] E. K. Irish, C. D. Ogden, and M. S. Kim, Phys. Rev. A **77**, 033801 (2008).
[16] O. Egorov and F. Lederer, Opt. Express **16**, 6050 (2008).
[17] S. Schmidt, D. Gerace, A. A. Houck, G. Blatter, and H. E. Türeci, Phys. Rev. B **82**, 100507 (2010).
[18] S. Ferretti, L. C. Andreani, H. E. Türeci, and D. Gerace, Phys. Rev. A **82**, 013841 (2010).
[19] D. K. Campbell, S. Flach, and Y. S. Kivshar, Phys. Today **57**, 43 (2004).
[20] F. Lederer, G. I. Stegeman, D. N. Christodoulides, G. Assanto, M. Segev, and Y. Silberberg, Phys. Rep. **463**, 126 (2008).
[21] D. Hennig and G. P. Tsironis, Phys. Rep. **307**, 333 (1999).
[22] D. Sarchi, I. Carusotto, M. Wouters, and V. Savona, Phys. Rev. B **77**, 125324 (2008).
[23] K. G. Lagoudakis, B. Pietka, M. Wouters, R. André, and B. Deveaud-Plédran, Phys. Rev. Lett. **105**, 120403 (2010).
[24] M. Albiez, R. Gati, J. Fölling, S. Hunsmann, M. Cristiani, and M. K. Oberthaler, Phys. Rev. Lett. **95**, 010402 (2005).
[25] S. Flach and C. R. Willis, Phys. Rep. **295**, 181 (1998).
[26] A. R. Bishop, G. Kalosakas, and K. O. Rasmussen, Chaos **13**, 558 (2003).
[27] G. P. Tsironis and S. Aubry, Phys. Rev. Lett. **77**, 5225 (1996).
[28] T. Kottos and M. Weiss, Phys. Rev. Lett. **93**, 190604 (2004).
[29] R. Livi, R. Franzosi, and G.-L. Oppo, Phys. Rev. Lett. **97**, 060401 (2006).
[30] E. M. Graefe, H. J. Korsch, and A. E. Niederle, Phys. Rev. Lett. **101**, 150408 (2008).
[31] G. S. Ng, H. Hennig, R. Fleischmann, T. Kottos, and T. Geisel, New J. Phys. **11**, 073045 (2009).
[32] S. M. Spillane, T. J. Kippenberg, O. J. Painter, and K. J. Vahala, Phys. Rev. Lett. **91**, 043902 (2003).
[33] M. Borselli, T. Johnson, and O. Painter, Opt. Express **13**, 1515 (2005).
[34] S. V. Boriskina, Opt. Lett. **31**, 338 (2006).
[35] S. V. Boriskina, Opt. Express **15**, 17371 (2007).
[36] P. M. Morse and H. Feshbach, *Methods of Theoretical Physics*, Vol. 1 (McGraw-Hill, New York, 1953).
[37] O. Zaitsev and L. Deych, J. Opt. **12**, 024001 (2010).
[38] H. E. Türeci, A. D. Stone, and B. Collier, Phys. Rev. A **74**, 043822 (2006).
[39] S. Prasad and R. J. Glauber, Phys. Rev. A **82**, 063805 (2010).
[40] Y. K. Chembo and N. Yu, Phys. Rev. A **82**, 033801 (2010).
[41] M. Abramowitz and I. Stegun, *Handbook of Mathematical Functions with Formulas, Graphs and Mathematical Tables* (US Government Printing Office, Washington, DC, 1964).
[42] P. Barclay, K. Srinivasan, and O. Painter, Opt. Express **13**, 801 (2005).
[43] M. L. Gorodetsky, A. D. Pryamikov, and V. S. Ilchenko, J. Opt. Soc. Am. B **17**, 1051 (2000).